

Preparation of $\text{Zn}_3\text{Ga}_2\text{Ge}_2\text{O}_{10}:\text{Cr}^{3+}$, Al^{3+} nanometer phosphors via sol-gel method

M. Y. Wu, Y. Wang, Y. Shen*, F. F. Li, J. Wang, Y. Liu, C. Peng

Key Laboratory of Environment Functional Materials of Tangshan City, Hebei Provincial Key Laboratory of Inorganic Nonmetallic Materials, College of Materials Science and Engineering, North China University of Science and Technology, Tangshan 063210, Hebei, China

In this paper, the near-infrared luminescence $\text{Zn}_3\text{Ga}_2\text{Ge}_2\text{O}_{10}:\text{Cr}^{3+}$, Al^{3+} prepared by citrate sol-gel method is studied. When the Cr^{3+} doping amount is 0.01% and the Al^{3+} doping amount is 0.2, the prepared $\text{Zn}_3\text{Ga}_2\text{Ge}_2\text{O}_{10}$: The afterglow properties of Cr^{3+} , Al^{3+} afterglow nanomaterials are the best. The sample has the least heterogeneous phase, the highest crystallinity, the longest afterglow time, the excitation peak at 267 nm and the emission peak at 745 nm. The light produced belongs to the wavelength range of near-infrared light. After excitation with an ultraviolet lamp, the material can see deep cherry red light in the dark.

(Received September 14, 2020; Accepted April 4, 2021)

Keyword: $\text{Zn}_3\text{Ga}_2\text{Ge}_2\text{O}_{10}:\text{Cr}^{3+}$, Al^{3+} , Afterglow materials, Sol-Gel Method, Luminescence properties

1. Introduction

Long afterglow Phosphors are simply referred to as long afterglow materials, also known as light-storing luminescent materials, luminous materials, which are essentially photoluminescent materials[1] that are capable of absorbing energy such as visible light, ultraviolet light, X-Ray and so on, and can continue to emit light after the excitation stops, it can store energy in energy traps, is a material with broad application prospects. The near-infrared long-lasting phosphor material is a long-lasting phosphor material in the infrared/near-infrared (700-780 nm) range. ZnGa_2O_4 is widely used as an important luminescent material in field emission display fields, such as electroluminescent displays and vacuum fluorescent displays [2-6]. Because they are more chemically stable than sulfide phosphors, they can withstand high beam currents[7]. The bandgap energy of ZnGa_2O_4 is 4.4 eV. After being excited by ultraviolet light and low voltage electrons, ZnGa_2O_4 emits strong blue light. This is achieved by the activation of the central GaO group[8-10]. Its luminescence properties can be adjusted by doping with transition metal or rare earth ions. Under the irradiation of ultraviolet light, $\text{ZnGa}_2\text{O}_4:\text{Cr}^{3+}$ can produce significant red long afterglow luminescence [11-17]. However, the red long-lasting luminescence properties of ZnGa_2O_4 are not ideal, and the incorporation of Ge or Si into the matrix can generate more

* Corresponding authors: shenyilzt@163.com

effective traps and enhance the remaining luminescence properties. Therefore, the properties of near-infrared luminescent $\text{Zn}_3\text{Ga}_2\text{Ge}_2\text{O}_{10}:\text{Cr}^{3+}, \text{Al}^{3+x}$ ($x=0,0.1,0.2,0.3$) nano long-lasting materials prepared by the citric acid sol-gel method have been studied. Improve the remaining Hui performance.

2. Experimental

2.1. Materials synthesis

According to the stoichiometric ratio, GeO_2 was accurately weighed in dilute ammonia water, and then $\text{Ga}(\text{NO}_3)_3 \cdot 8\text{H}_2\text{O}$, $\text{Al}(\text{NO}_3)_3 \cdot 9\text{H}_2\text{O}$, $\text{Zn}(\text{NO}_3)_2 \cdot 6\text{H}_2\text{O}$, $\text{Cr}(\text{NO}_3)_3 \cdot 9\text{H}_2\text{O}$ were weighed according to the stoichiometric ratio. respectively, dissolved in an appropriate amount of deionized water to fully mix, after stirring evenly, according to the amount of total metal ions and citric acid substances 1:1.5 added citric acid aqueous solution and stirred uniformly, the mixture was added Ge^{4+} solution; fully diluted with diluted ammonia The pH of the mixed solution was adjusted to 5 and stirred on a magnetic stirrer for 2 hours to form a sol; the sol was dried at 75°C and dried at 130°C to form a dry gel. The xerogel was carbonized at 200°C for 7 h to obtain a black porous powder. The powder was heat-treated at 1000°C and held for 3 h.

2.2. Characterization methods

The crystal composition of the sample was measured using a D/MAX2500PC type X-ray diffractometer (XRD) from Japan Science and Technology Co., Ltd. ($\text{Cu K}\alpha$, 10° to 80°); the sample afterglow performance was measured by a Hitachi Instruments F-700FL fluorescence spectrophotometer and had afterglow performance. The material, after the light has stopped, can also keep emitting light for a certain period of time, and the intensity of the emitted light gradually weakens until it disappears. This process is the process of attenuation. The experiment uses the afterglow decay curve to analyze the luminescence properties of the sample. The fluorescence spectrum includes two large parts of the excitation and emission spectra. The emission spectrum of a sample is drawn by exciting a certain material with a certain wavelength of light, making the material luminesce, and then in accordance with the intensity of light emitted by the material and the distribution of energy.

3. Results and discussion

3.1 TG-DTA analysis

In this experiment, the factors affecting the morphology and afterglow properties of $\text{Zn}_3\text{Ga}_2\text{Ge}_2\text{O}_{10}:\text{Cr}^{3+}, \text{Al}^{3+}$ afterglow nanomaterials are considered as raw material ratio, pH value, calcining temperature and holding time. In order to determine the reasonable range of various factors, the TG-DTA analysis of $\text{Zn}_3\text{Ga}_2\text{Ge}_2\text{O}_{10}:\text{Cr}^{3+}, \text{Al}^{3+}$ afterglow nanomaterials synthesized by sol-gel method was first performed, as shown in Fig. 1.

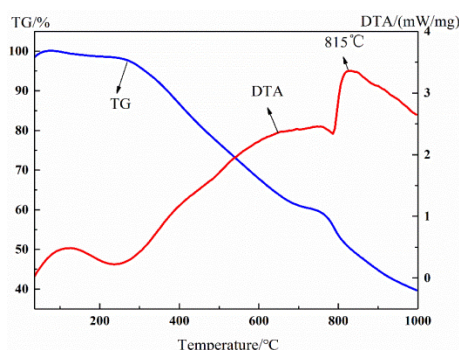


Fig. 1. TG-DTA curves of presoma.

Fig. 1 shows the TG-DTA thermal analysis of precursors after carbonization of $\text{Zn}_3\text{Ga}_2\text{Ge}_2\text{O}_{10}:\text{Cr}^{3+}$, Al^{3+} afterglow nanomaterials synthesized by sol-gel method. From the figure, it can be seen that at 300-750°C, the corresponding TG curve decreases rapidly and the quality of the system decreases rapidly. This may be due to the reaction of carbon and oxygen in the carbonized precursor, and the generated CO is continuously removed. At this time, the system quality the decrease was 58.94%. In addition, with the increase of temperature, a wide exothermic peak with a peak value of 815°C appeared at 800-1000°C. This was due to the formation of the $\text{Zn}_3\text{Ga}_2\text{Ge}_2\text{O}_{10}$ crystal structure. The two exothermic peaks appearing during the reaction are all gentle. This may be due to the slower heating rate, because the heating rate is small and the crystal can grow fully.

Based on the above analysis, the temperature raising system established in this experiment is: from room temperature to 5 °C/min to 550 °C, heat for 60 min, then increase to 3 °C/min to 1000 °C for 3 h, cooling in the air.

3.2. SEM analysis

Fig. 2 is a SEM of $\text{Zn}_3\text{Ga}_2\text{Ge}_2\text{O}_{10}:\text{Cr}^{3+}$, Al^{3+} afterglow nanomaterials at a calcination temperature of 1000 °C. The sample is a relatively uniform sphere with a particle size of approximately 80 nm and is a nanomaterial. The grains did not agglomerate and the morphology of the sample was better.

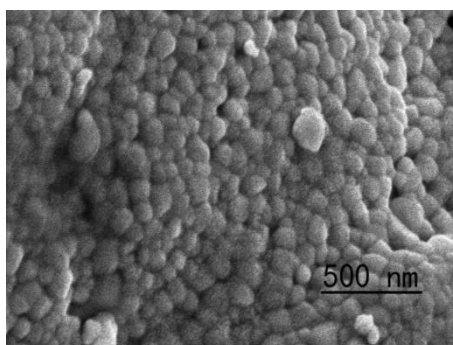


Fig. 2. SEM images of the $\text{Zn}_3\text{Ga}_2\text{Ge}_2\text{O}_{10}:\text{Cr}^{3+}$, Al^{3+} afterglow nanomaterial.

3.3. XRD analysis

Fig. 3 shows the XRD patterns of $\text{Zn}_3\text{Ga}_2\text{Ge}_2\text{O}_{10}:\text{Cr}^{3+}, \text{Al}^{3+}$ afterglow nanomaterials with different Al^{3+} contents. Through analysis, it can be obtained that the samples prepared at the three Al^{3+} doping amounts have formed $\text{Zn}_3\text{Ga}_2\text{Ge}_2\text{O}_{10}:\text{Cr}^{3+}, \text{Al}^{3+}$, and the formed hetero-phases are few. There is a very small amount of diffraction peaks of GeO_2 in the sample because GeO_2 is insoluble in water and is formed when the gel is prepared. A small amount of diffraction peaks of ZnO appeared in the sample, which may be due to the fact that Zn^{2+} forms an insoluble zinc hydroxide in an alkaline environment and decomposes to form ZnO and H_2O during the heating process.

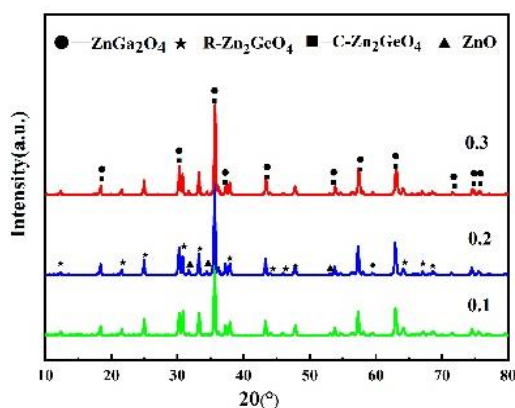


Fig. 3. XRD pattern of $\text{Zn}_3\text{Ga}_2\text{Ge}_2\text{O}_{10}:\text{Cr}^{3+}, \text{Al}^{3+}$ with different dosage of Al^{3+} .

3.4. Photoluminescence properties

Fig. 4 shows the excitation emission spectra of Cr^{3+} and Al^{3+} doped $\text{Zn}_3\text{Ga}_2\text{Ge}_2\text{O}_{10}$ samples. It can be seen from the figure that the four Al^{3+} doping amounts have no significant effect on the shape and position of the excitation and emission peaks, but differ in intensity, and the excitation and emission peaks have the highest intensities when the Al^{3+} doping percentage is 0.2. The excitation peak at 267 nm can be excited, and its emission peaks are all 745 nm, belonging to the wavelength range of near-infrared light. After being excited with ultraviolet light, the $\text{Zn}_3\text{Ga}_2\text{Ge}_2\text{O}_{10}:\text{Cr}^{3+}, \text{Al}^{3+}$ afterglow nanomaterial emits dark cherry red in the dark bright.

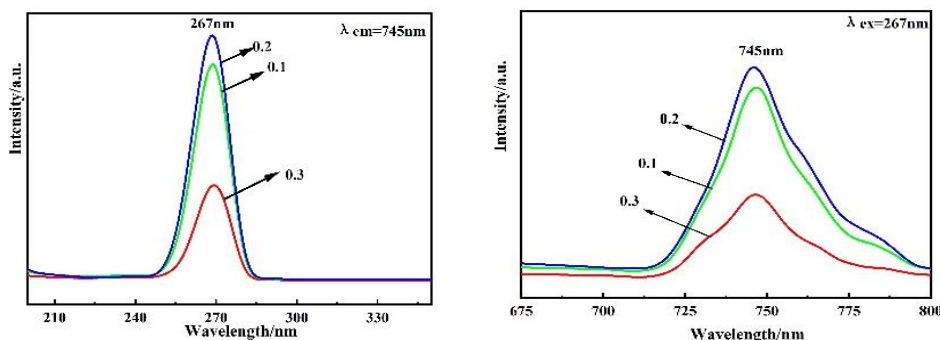


Fig. 4. (a) Excitation and (b) emission spectra recorded of $\text{Zn}_3\text{Ga}_2\text{Ge}_2\text{O}_{10}:\text{Cr}^{3+}, \text{Al}^{3+}$ with different dosage of Al^{3+} .

3.5. Long afterglow properties

In order to further observe the afterglow properties of the samples, an afterglow decay curve was plotted for the Cr^{3+} , Al^{3+} doped $\text{Zn}_3\text{Ga}_2\text{Ge}_2\text{O}_{10}$ samples prepared by the sol-gel method, as shown in Fig.5. The afterglow properties of $\text{Zn}_3\text{Ga}_2\text{Ge}_2\text{O}_{10}:\text{Cr}^{3+}$, Al^{3+} afterglow nanomaterials were best when the Al^{3+} doping percentage was 0.2. The afterglow properties of the samples were the next when the Al^{3+} doping percentage was 0.1, and the afterglow properties of the samples when the Al^{3+} doping percentage was 0.3. Worst.

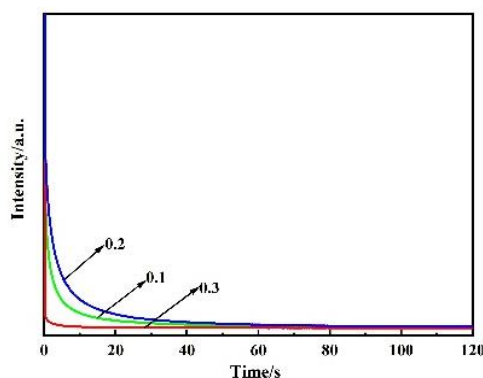


Fig. 5. Decay curves of $\text{Zn}_3\text{Ga}_2\text{Ge}_2\text{O}_{10}:\text{Cr}^{3+}$, Al^{3+} with different dosage of Al^{3+} .

4. Conclusion

When $\text{Zn}_3\text{Ga}_2\text{Ge}_2\text{O}_{10}:\text{Cr}^{3+}$, Al^{3+} nano long afterglow material was prepared by sol-gel method, the Cr^{3+} doping amount was 0.01%, and the Al^{3+} doping amount was 0.2, the obtained afterglow properties of $\text{Zn}_3\text{Ga}_2\text{Ge}_2\text{O}_{10}:\text{Cr}^{3+}$, Al^{3+} afterglow nanomaterials were best. The afterglow is the longest. The excitation peak is at 267 nm and the emission peak is at 745 nm. It belongs to the wavelength range of near-infrared light. After being excited with ultraviolet light, the material emits dark cherry red light in darkness.

Acknowledgements

This work was supported by the National Natural Science Fund of China(Grant No. 51772099, 51572069, 51872091), Scientific and Technological Research Projects of Colleges and Universities in Hebei Province(QN2019049), the Doctoral Initiation Fun(BS2017025)and Innovation and Entrepreneurship Training Program for College Students of North China University of Science and Technology.

References

- [1] T. Matsuzawa, Y. Aoki, N. Takeuchi et al., *Journal of the Electrochemical Society* **144**(9), 243 (1996).
- [2] F. Shen, C. Deng, X. Wang et al., *Materials Letters* **178**, 185 (2016).
- [3] F. Shen, J. Xia, Z. Cheng, *China Light & Lighting* **11**(2), 9 (2016).
- [4] A. Bessi Re, A. Lecointre, B. Viana et al., *Optics Express* **19**(11), 10131 (2011).
- [5] X. Duan, J. Liu, Y. Wu et al., *Journal of Luminescence* **153**(3), 361 (2014).
- [6] D. Li, Y. Wang, K. Xu et al., *Optical Materials* **42**, 313 (2015).
- [7] Y. Wu, L. Yang, X. Qin et al., *Spectrochimica Acta Part A Molecular & Biomolecular Spectroscopy* **151**(6), 385 (2015).
- [8] F. Shen, C. Deng, X. Wang et al., *Journal of Materials Science: Materials in Electronics* **27**(9), 1 (2016).
- [9] J. Li, J. Shi, J. Shen et al., *Nano-Micro Letters* **7**(2), 138 (2015).
- [10] I. P. Sahu, D. P. Bisen, R. K. Tamrakar et al., *Research on Chemical Intermediates* **42**(3), 1823 (2016).
- [11] K. Shinozaki, T. Honma, M. Affatigato et al., *Journal of Luminescence* **177**, 286 (2016).
- [12] J. Liang, Y. Q. Cao, H. Lin, Z. Z. Zhang, C. C. Huang, X. X. Wang, *Inorg. Chem.* **52**, 6916 (2013).
- [13] S. C. Yan, J. J. Wang, H. L. Gao, N. Y. Wang, H. Yu, Z. S. Li, Y. Zhou, Z. G. Zou, *Adv. Funct. Mater.* **23**, 758 (2013).
- [14] K. Maeda, *J. Photochem. Photobiol. C* **12**, 237 (2011).
- [15] A. Abdullah, M. Anis-Ur-Rehman, A. S. Saleemi, et al., *Digest Journal of Nanomaterials and Biostructures* **14**(3), 667 (2019).
- [16] X. Duan, J. Liu, Y. Wu et al., *Journal of Luminescence* **153**(3), 361 (2014).
- [17] K. Somasundaram, K. P. Abhilash, V. Sudarsan et al., *Physica B: Condensed Matter* **491**, 79 (2016).